Interlocking of heterogeneous plate coupling and aftershock area expansion pattern for the 2011 Tohoku-Oki Mw9 earthquake

Fumiko Tajima[1] and Brian L. N. Kennett[2]

Received 20 December 2011; revised 2 February 2012; accepted 7 February 2012; published 6 March 2012.

[1] The 2011 Tohoku-Oki earthquake (Mw9.0) ruptured a large portion of the plate boundary where the coupling was considered weak and represented by sparsely distributed small asperities. A typical asperity break produced an event of around Mw7.5 accompanied by a subsequent expansion of aftershock activity beyond the main rupture zone. Unlike previous large earthquakes, the Mw9.0 earthquake sequence does not show much spatial expansion of aftershock activity, but the areas of slip deficit in the main rupture zone are progressively filled in by aftershocks. We show a clear image of segmentation of physical properties in the subducted slab that has been revealed by joint tomography of P and S wave arrivals. The mapped variations separate the zones of dominant high-frequency radiation down-dip and dominant low-frequency radiation up-dip on the mainshock fault. These changes indicate significant variations in the effective plate coupling that interlocked the source areas of the past distinct earthquakes. **Citation:** Tajima, F., and B. L. N. Kennett (2012), Interlocking of heterogeneous plate coupling and aftershock area expansion pattern for the 2011 Tohoku-Oki Mw9 earthquake, *Geophys. Res. Lett.*, *39*, L05307, doi:10.1029/2011GL050703.

1. Introduction

[2] Over the last few decades an asperity model [*Ruff and Kanamori*, 1980, 1983; *Lay and Kanamori*, 1981; *Lay et al.*, 1982] has been developed to characterize the ruptures of large shallow subduction zone earthquakes in context of the strength of plate coupling. The 2011 Tohoku-Oki earthquake (moment magnitude, Mw 9.0) ruptured a large portion of the boundary between the subducting Pacific and the overriding Okhotsk plates where the coupling was considered weak and represented by sparsely distributed small asperities [e.g., *Tajima and Kanamori*, 1985a, 1985b] so that such a great earthquake had not been anticipated. In the region off the coast of Miyagi-prefecture in northeast (NE) Japan an earthquake of a magnitude (M) around Mw7.5 was expected with a recurrence interval of 30–40 years based on the past activity over the last 150 years.

[3] Two days before the great 2011 March 11 earthquake, an Mw7.3 event occurred on the same subduction zone, somewhat further offshore than the anticipated event. A spokesman on a television news program warned that the aftershock activity could last with events of M > 6 for a week or so, presumably based on the assumption that it should decrease with time as represented by the Modified Omori law [*Utsu*, 1961]. Such a formulation does not account for the spatial extent of the affected area. The March 9 event turned to be a mere foreshock to the Mw9.0 March 11 earthquake that released about 180 times as much energy as an Mw7.5 event, and produced several dozens of aftershocks of M > 6. In reality we only learn whether we have a *foreshock, mainshock or aftershock,* after the sequence, and did not know in advance the nature of the driving force that controls the propagation of seismic rupture that ended up as an Mw9 event.

[4] This 2011 megathrust earthquake is one of the greatest ever instrumentally recorded, comparable to the 1960 Chilean (Mw9.5), the 1964 Alaskan (Mw9.2) and the 2004 Sumatra-Andaman (Mw9.0-9.3) events. The previous major earthquake catastrophe in Japan was the 1995 Kobe disaster (Mw6.8). Since then, Japan has installed one of the world's densest real-time seismometer monitoring systems, and the most extensive earthquake early-warning system. The excellent distribution of seismic stations and plentiful earthquake sources allow the production of high resolution seismic tomography models and models for seismic rupture. The advances in the available information have been very significant. Nonetheless, the potential for an impending Mw9 earthquake was not broadly recognized, although analysis of earlier events suggested that only a fraction of the accumulated tectonic stress was being relieved, and that there was indeed a possibility of an event that combined near-trench and near coast slips that in the past few centuries had only occurred in distinct earthquakes [*Igarashi et al.*, 2003; *Kanamori et al.*, 2006].

2. Plate Coupling and Aftershock Expansion Pattern

[5] In the aftermath of a seismic event there is an expansion of aftershock activity reflecting stress adjustment outside the ruptured areas. A simple tool has been developed to characterize the spatial expansion patterns of aftershocks with time, based upon the amount of seismic energy released from aftershocks per unit area and unit time [*Tajima and Kanamori*, 1985a]. A linear expansion ratio η_l for the characteristic size of the aftershock zone and an areal expansion ratio η_S are calculated as a function of time. The ratios are calculated from the size at a certain time after the mainshock t_{aft}(day) divided by that at 1-day, since the 1-day aftershock area is considered to represent the rupture of an asperity. The results indicate that typical expansion patterns of aftershock areas for major subduction events can be classified into three groups [*Tajima and Kanamori*, 1985b]: (1) very little

[1]Department of Earth and Environmental Sciences, Ludwig-Maximilians-University, Munich, Germany.
[2]Research School of Earth Sciences, Australian National University, Canberra, ACT, Australia.

0094-8276/12/2011GL050703

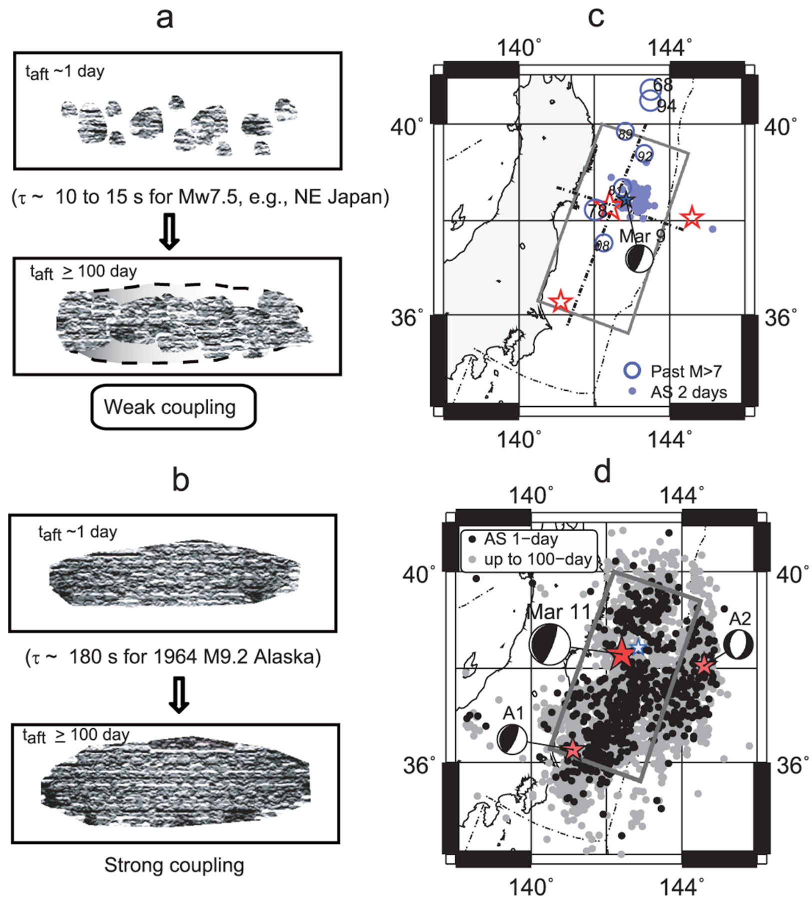

Figure 1. Illustration of two typical aftershock area expansion patterns associated with the asperity distribution and the aftershock activity of the 2011 Tohoku-Oki earthquake. (a) The plate coupling is characterized by sparsely distributed small asperities, and considered weak like in NE Japan. The aftershock area at a small t_{aft} ($\sim$1 day) is identified as an asperity. Aftershock areas expand into the surrounding areas significantly at a large t_{aft}, ($\geq$100 days) often overlapping that of an adjacent major event. A typical large source rupture has a characteristic time τ of 10 to 15 s. (b) A fault zone is characterized with a uniform, large asperity. The aftershock area does not expand much at a large t_{aft} and the interplate coupling is considered strong such as in the Alaskan subduction zone. The source-process time τ of the 1964 Alaska earthquake (Mw9.2) was $\sim$180 s. (c) The immediate aftershocks of the Mw7.3 event on March 9th are located mainly to the east of the epicenter (light blue star). Large earthquakes (M $\geq$ 7) in the past half century are also shown (open circles in light violet). The ruptured area of the March 11th event is outlined by a grey rectangle. The red open stars indicate the epicenters of the Mw9 event and two large aftershocks (M > 7) on March 11th (A1 and A2 in Figure 1d). (d) The Mw9 earthquake and its aftershocks: for 1-day (solid black circles) and for the period up to t_{aft} =100 days (grey shaded circles). Both $\eta_l(100)$ and $\eta_s(100)$ are less than 1.5 that are similar to those of a megathrust event in Alaska.

expansion associated with a megathrust earthquake, e.g., the 1964 Alaskan earthquake (Mw9.2); (2) little expansion along the strike and some expansion widthwise, e.g., large events in the Kurile subduction zone; (3) large areal and linear expansions, e.g., 1968 Tokachi-oki (Mw8.2), 1978 Miyagi-oki (Mw7.5) in the NE Japanese subduction zone.

[6] The plate coupling in NE Japan is characterized by sparsely distributed small asperities, each of which could produce an event of Mw$\sim$7.5 to lower 8 (Figure 1a). A typical asperity break shows a complex source rupture process [e.g., *Seno et al.*, 1980], but the driving force of rupture propagation may not be large enough to break through a broad region, as was in the case in the 2011 Mw9 earthquake. The weaker zones surrounding the asperities are likely to be broken by smaller events, aftershocks or repeating small events [*Matsuzawa et al.*, 2002; *Igarashi et al.*, 2003]. The aftershock activity expands significantly into the surrounding areas (asperity group-3). This pattern is in contrast to a fault zone that is characterized by a uniform, large asperity, the rupture of which could produce a megathrust event, e.g., the 1964 Alaska earthquake with a characteristic source-time τ of $\sim$180 s (group-1). The aftershock area does not show much expansion at $t_{aft}\sim$large ($\geq$100 days) (Figure 1b) and the inter-plate coupling is considered strong.

[7] The rupture pattern of the 2011 Tohoku-Oki earthquake sequence that started with the Mw7.3 foreshock is compared with the patterns postulated previously for this region. The 2-day aftershock area of the March 9 foreshock mainly expanded trenchward until the March 11th event took place at the western edge of the zone (Figure 1c). It seems there is a distinct zone with a strong coupling strength associated with a nucleation of the Mw9 megathrust event. After the March 11 earthquake ruptured the broad region in $\tau \sim 150$ s, however, the aftershock area did not

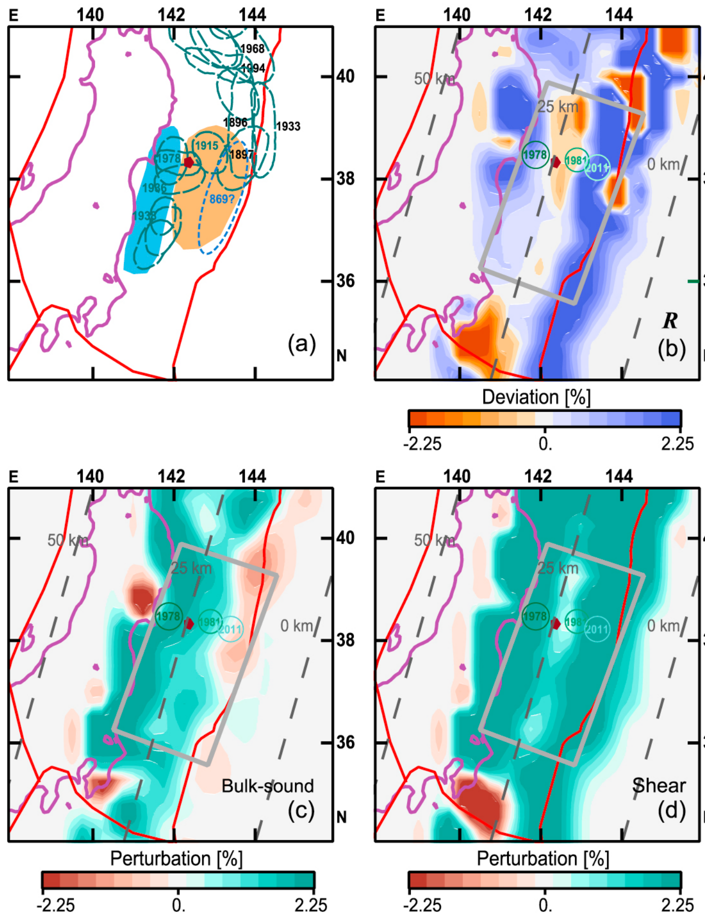

Figure 2. Multiple images of the rupture area of the 2011 Tohoku-Oki event. (a) The locations of the zones of dominant high-frequency radiation (light blue) and dominant low-frequency energy radiations (buff) with the inferred rupture area of past large earthquakes superimposed. (b) The joint tomographic image for the ratio R on an inclined plane with the depths indicated by dashed lines at 0, 25, and 50 km through the upper part of the subduction zone; reference point: 142°E, 38°N, 25 km depth, plane with dip azimuth 195°, dip angle 10°. The source area for the March 11 mainshock is outlined by a grey rectangle. The locations of the recent events (1978, 1981, 2011 March 9) are indicated together with the hypocenter of the March 11 event (red pentagon). (c) Bulk-sound speed tomographic image taken along the same inclined plane. (d) Shear wave speed tomographic image taken along the same inclined plane. Each of the tomographic quantities has been separately interpolated on to the inclined plane from the 3-D models, so there can be slight differences from direct construction of the fields on the plane.

show much expansion over time as compared with the 1-day area in spite of the numerous aftershocks (Figure 1d). Unlike the previous large earthquakes in this subduction zone, this expansion pattern is similar to that of asperity group-1 (Figure 1b). Here we consider the aftershock area to be linked to the main rupture zone, and the large events (M > 6) in Niigata or Shizuoka, which were apparently induced after March 11 as a separate feature.

3. Joint Seismic Tomography Image

[8] Models for the 2011 March 11 source rupture show notable differences depending on the specific source of information employed [*Furumura et al.*, 2011; *Ide et al.*, 2011; *Koketsu et al.*, 2011; *Lay et al.*, 2011; *Simons et al.*, 2011; *Wang and Mori*, 2011a, 2011b]. However, a consistent feature is the separation of areas associated with dominant high- and low-frequency radiation down-dip and up-dip from the hypocenter (Figure 2a). A recent joint seismic tomography model using both P and S wave arrivals provides an indication of variations in physical properties in the subducting plate [*Gorbatov and Kennett*, 2003; *Kennett et al*, 2011]. In the old subducting Pacific plate in the Japan area, shear wavespeed variations ($\delta\beta/\beta$) dominate variations in bulk-sound speed ($\delta\phi/\phi$) (the wavespeed associated with bulk-modulus alone). The variations in the wavespeed structure can be enhanced by examining a measure (R) [*Kennett et al*, 2011] of the relative variations in $\delta\phi/\phi$ and $\delta\beta/\beta$ with respect to the *ak135* reference model [*Kennett et al*, 1995].

$$R = \frac{1 + {}^{\delta\beta}/_{\beta}}{1 + {}^{\delta\phi}/_{\phi}} - 1, \qquad (1)$$

where the seismic wavespeeds are given by $\beta^2 = G/\rho$, $\phi^2 = K_S/\rho$, in terms of the shear modulus G, bulk-modulus K_S, and density ρ. To first order, the measure R is simply the

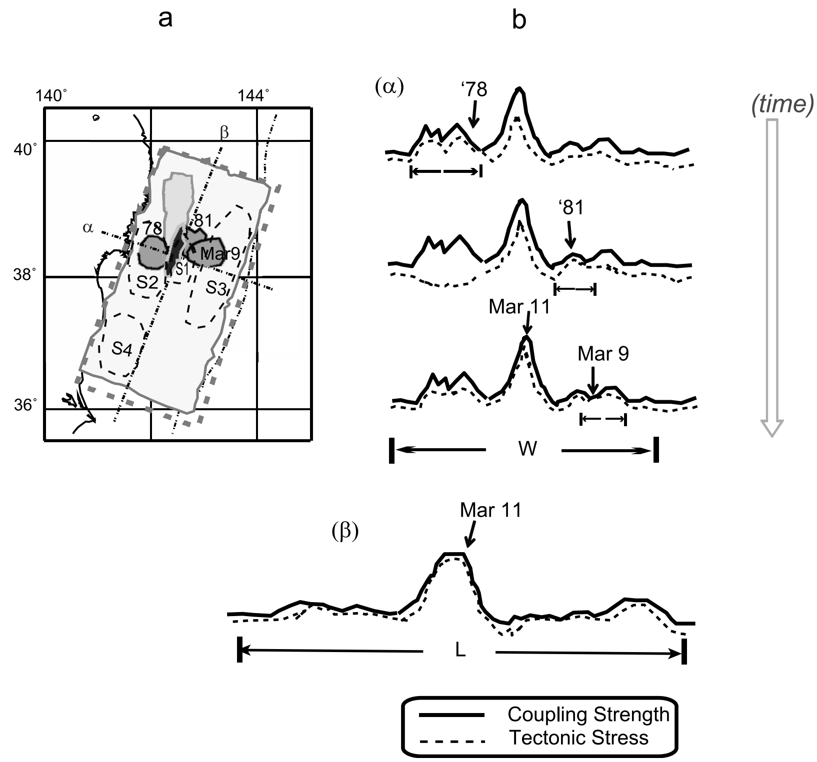

Figure 3. Conceptual model of effective plate coupling strength and progressive tectonic stress. (a) The asperities which caused the 1978 (Mw7.5), 1981 (Mw7.1), and March 9th (Mw7.3) events are illustrated by dark shading. The area in lighter shade extending to the north corresponds to the zone with R < 0, with a superposed black zone to show the initiation of the March 11 mainshock. See the text for the explanation of S1, S2, S4, and S3 (indicated by dotted ellipses). The dashed rectangle corresponds to the fault area shown in Figure 2b. (b) Illustration of the heterogeneous plate coupling strength (solid line) and the progressive tectonic shear stress level (dashed line) associated with the earthquakes in 1978, 1981, and March 2011 along cross sections α and β in Figure 3a. Here the scales are arbitrary with some exaggeration.

difference ($\delta\beta /\beta - \delta\phi /\phi$) and so enhances the subtle differences in the behavior of the shear and bulk moduli, since the density ρ is common to both wavespeeds.

[9] Tomographic images are taken on a plane approximately coincident with the fault surface. *R* shows a distinct reduction to zero and slightly negative values (light orange) just up-dip of the mainshock hypocenter (Figure 2b). The down-dip edge of this zone corresponds to the separation between the regions of dominant high-frequency radiation and dominant low-frequency radiation. The March 9 foreshock lies just outside the anomalous zone, as does the 1978 Mw7.5 event. In the lower two panels the images for $\delta\phi/\phi$ and $\delta\beta/\beta$ are shown separately. There is a significant gradient in $\delta\phi/\phi$, a slight negative anomaly near the trench, which then grades to stronger positive anomalies at depth (Figure 2c). In contrast $\delta\beta/\beta$ is generally strongly positive with just a slight reduction at depths near 25 km, the hypocentral depth of the March 11 event (Figure 2d). The zone of reduced *R* is largely associated with this reduction in $\delta\beta/\beta$ with the effects enhanced by the increase in $\delta\phi/\phi$, and appears to have a strong influence on plate coupling over the whole of the rupture area. The edges of the anomalous region we have delineated act as the initiation points for rupture process of the March 2011 sequence as well as for 1978 (Mw7.5) and 1981 (Mw7.0) events (Figure 2a), and these locations will be where the strongest contrasts exist in physical properties. Regional P wave tomography [*Zhao et al.*, 2011] indicates additional significant wavespeed variations above the slab interface that could affect the frictional properties at the plate boundary.

[10] To the south of rupture zone of the 2011 Tohuku event, we note a further anomaly in *R*, but in this case we have strong reductions in both the bulk-sound speed and shear wavespeed, a very different configuration from further north. In the study of *Loveless and Meade* [2010] this southern zone shows a very different style of plate coupling to the locked area to the north. Once again it appears that structural information can provide useful indications of the state of the subduction system.

[11] A seemingly robust approach [*Ide et al.*, 2011] used the Mw7.3 foreshock as an empirical Green's function exploiting the similar focal mechanisms and location proximity, and determined the mainshock source process with the features that consist of a small initial phase (area S1 near the hypocenter), deep rupture radiating high frequency energy for up to 40 s (S2), extensive shallow rupture at 60 to 70 s with relatively low-frequency energy radiation (S3), and continuing deep rupture lasting more than 100 s (S4). A unified source model [*Koketsu et al.*, 2011] combining results of many different types, delineates the large slip in the up-dip zone that creates the seafloor movement and tsunami. The presence of the significant R anomaly at the trench line may well be linked to the large coseismic slip. However, we have to be cautious in any interpretation of the

very shallowest features since they are likely to have a strong dependence on the event locations used in the tomographic inversion and the particular slice through the model. The tomography image [*Gorbatov and Kennett*, 2003], created prior to 2003, indicates significant clues to the impending March 2011 rupture process.

4. Interlocking of Effective Plate Coupling

[12] In the light of the results above, we attempt to formulate a conceptual model of rupture propagation at the subducting plate interface in NE Japan. The distribution of plate coupling strength (or asperities) is illustrated in Figure 3a. The asperities which caused the 1978, 1981, and 2011 March 9 earthquakes are illustrated by dark shading. The area in lighter shade extending to the north corresponds to the zone with $R < 0$, on which the black zone is superposed to show the initiation of the March 11 mainshock. The edges of the distinct rupture zones are expected to have localized stress concentrations that are relieved in the aftershock activity. Expansions of the aftershock areas have occurred where the stress concentrations migrate beyond the rupture zones of the past large earthquakes [*Tajima and Kanamori*, 1985a]. Nonetheless, the narrow area of the March 11 mainshock initiation remained intact until the tectonic stress level reached the maximum coupling strength there, which is higher than in the surrounding areas. As noted by *Lay et al.* [2011] the slip displacement for the same moment release is enhanced by the reduced seismic wavespeeds toward the trench. Thus comparable strength asperities can lead to much larger slip in the near trench zone as in zone S2.

[13] In Figure 3b the progressive tectonic stress level is drawn schematically in relation to the heterogeneous plate coupling strength associated with the major seismic ruptures since the 1978 earthquake. The distribution of the heterogeneous shear strengths represents the effective plate coupling for interlocking the distinct source areas. When the March 11 mainshock rupture started, the tectonic stress levels in the past distinct source areas were close to the maximum shear strength for these zones. This condition promoted interlocking rupture propagation through the broad region. On the other hand the set of ruptures during the mainshock removed the slip deficit on parts of the plate interface. The rupture gaps are progressively filled in by the aftershocks, particularly those of larger size that fit in the larger 'holes' in the main rupture slip distribution (Figures 1d and 3a).

[14] The combined exploitation of joint seismic tomography and seismic rupture patterns as used for the Tohoku-Oki earthquake may be utilized to extract clues for potential for future interlocking megathrust events (see the image of relative variations of $\delta\beta/\beta$ and $\delta\phi/\phi$ for the broader region around the Japan islands [*Kennett et al.*, 2011]).

[15] **Acknowledgments.** F.T. appreciates the supports and research environment provided at LMU. She has benefitted from instruction from the late Leon Knopoff who introduced her to the concept of a rupture driving force in heterogeneous plate coupling. Collaboration in Munich was made possible by Humboldt Foundation support to B.K. The review comments by an anonymous reviewer helped to improve the clarity of the paper. "GMT" [*Wessel and Smith*, 1995] was used to produce Figure 1.

[16] The Editor thanks the anonymous reviewer for their assistance in evaluating this paper.

References

Furumura, T., et al. (2011), Strong ground motions from the 2011 off-the Pacific-Coast-of-Tohoku, Japan (Mw = 9.0) earthquake obtained from a dense nationwide seismic network, *Landslide*, *8*, 333–338, doi:10.1007/s10346-011-0279-3.

Gorbatov, A., and B. L. N. Kennett (2003), Joint bulk-sound and shear tomography for western Pacific subduction zones, *Earth Planet. Sci. Lett.*, *210*, 527–543, doi:10.1016/S0012-821X(03)00165-1.

Ide, S., A. Baltay, and G. C. Beroza (2011), Shallow dynamic overshoot and energetic deep rupture in the 2011 *Mw* 9.0 Tohoku-oki earthquake, *Science*, *332*, 1426–1429, doi:10.1126/science.1207020.

Igarashi, T., T. Matsuzawa, and A. Hasegawa (2003), Repeating earthquakes and interplate aseismic slip in the northeastern Japan subduction zone, *J. Geophys. Res.*, *108*(B5), 2249, doi:10.1029/2002JB001920.

Kanamori, H., M. Miyazawa, and J. Mori (2006), Investigation of the earthquake sequence off Miyagi prefecture with historical seismograms, *Earth Planets Space*, *58*, 1533–1541.

Kennett, B. L. N., E. R. Engdahl, and R. Buland (1995), Constraints on seismic velocities in the Earth from travel times, *Geophys. J. Int.*, *122*, 108–124, doi:10.1111/j.1365-246X.1995.tb03540.x.

Kennett, B. L. N., A. Gorbatov, and E. Kiser (2011), Structural control on the Mw 9.0 2011 offshore-Tohoku earthquake, *Earth Planet. Sci. Lett.*, *310*, 462–467, doi:10.1016/j.epsl.2011.08.039.

Koketsu, K., et al. (2011), A unified source model for the 2011 Tohoku earthquake, *Earth Planet. Sci. Lett.*, *310*, 480–487, doi:10.1016/j.epsl.2011.09.009.

Lay, T., and H. Kanamori (1981), An asperity model of large earthquake sequences, in *Earthquake Prediction: An International Review*, *Maurice Ewing Ser.*, vol. 4, edited by W. Simpson and G. Richards, pp. 579–592, AGU, Washington, D. C., doi:10.1029/ME004p0579.

Lay, T., H. Kanamori, and L. Ruff (1982), The asperity model and the nature of large subduction zone earthquakes, *Earthquake Predict. Res.*, *1*, 3–71.

Lay, T., C. J. Ammon, H. Kanamori, L. Xue, and M. J. Kim (2011), Possible large near-trench slip during the great 2011 Tohoku (Mw 9.0) earthquake, *Earth Planets Space*, *63*, 687–692, doi:10.5047/eps.2011.05.033.

Loveless, J. P., and B. J. Meade (2010), Geodetic imaging of plate motions, slip rates, and partitioning of deformation in Japan, *J. Geophys. Res.*, *115*, B02410, doi:10.1029/2008JB006248.

Matsuzawa, T., T. Igarashi, and A. Hasegawa (2002), Characteristic small-earthquake sequence off Sanriku, northeastern Honshu, Japan, *Geophys. Res. Lett.*, *29*(11), 1543, doi:10.1029/2001GL014632.

Ruff, L., and H. Kanamori (1980), Seismicity and the subduction process, *Phys. Earth Planet. Inter.*, *23*, 240–252, doi:10.1016/0031-9201(80)90117-X.

Ruff, L., and H. Kanamori (1983), The rupture process and asperity distribution of three great earthquakes from long-period diffracted P-waves, *Phys. Earth Planet. Inter.*, *31*, 202–230, doi:10.1016/0031-9201(83)90099-7.

Seno, T., K. Shimazaki, P. Sommerville, K. Sudo, and T. Eguchi (1980), Rupture process of the Miyagi-oki, Japan, earthquake of June 12, 1978, *Phys. Earth Planet. Inter.*, *23*, 39–61, doi:10.1016/0031-9201(80)90081-3.

Simons, M., et al. (2011), The 2011 magnitude 9.0 Tohoku-oki earthquake: Mosaicking the megathrust from seconds to centuries, *Science*, *332*, 1421–1425, doi:10.1126/science.1206731.

Tajima, F., and H. Kanamori (1985a), Global survey of aftershock area expansion patterns, *Phys. Earth Planet. Inter.*, *40*, 77–134, doi:10.1016/0031-9201(85)90066-4.

Tajima, F., and H. Kanamori (1985b), Aftershock area expansion and mechanical heterogeneity of fault zone within subduction zones, *Geophys. Res. Lett.*, *12*, 345–348, doi:10.1029/GL012i006p00345.

Utsu, T. (1961), A statistical study on the occurrence of aftershocks, *Geophys. Mag.*, *30*, 521–605.

Wang, D., and J. Mori (2011a), Rupture process of the 2011 off the Pacific coast of Tohoku earthquake (Mw 9.0) as imaged with back-projection of teleseismic P-waves, *Earth Planets Space*, *63*, 603–607, doi:10.5047/eps.2011.05.029.

Wang, D., and J. Mori (2011b), Frequency-dependent energy radiation and fault coupling for the 2010 Mw8.8 Maule, Chile, and 2011 Mw9.0 Tohoku, Japan, earthquakes, *Geophys. Res. Lett.*, *38*, L22308, doi:10.1029/2011GL049652.

Zhao, D., Z. Huang, N. Umino, A. Hasegawa, and H. Kanamori (2011), Structural heterogeneity in the megathrust zone and mechanism of the 2011 Tohoku-oki earthquake (Mw 9.0), *Geophys. Res. Lett.*, *38*, L17308, doi:10.1029/2011GL048408.

B. Kennett, Research School of Earth Sciences, Australian National University, Mills Road, Canberra, ACT 0200, Australia.

F. Tajima, Department of Earth and Environmental Sciences, Ludwig-Maximilians-University, Theresienstrasse 41, D-80333 München, Germany. (tajima@geophysik.uni-muenchen.de)